A New Transmitter-Receiver Architecture for Noncoherent Multirate OFFH-CDMA System with Fixed Optimal Detection Threshold

Elie Inaty, Hossam M. H. Shalaby, and Paul Fortier
Department of Electrical and Computer Engineering
Laval University, Québec, Canada G1K 7P4

***Abstract*—This paper analyses a new transmitter-receiver architecture based on a modified version of unipolar-bipolar correlation proposed for noncoherent multirate optical fast frequency hopping CDMA (OFFH-CDMA) system. The system assigns a frequency-shifted version (FSV) of the code used to transmit data bit "1" in order to transmit data bit "0". For the original system, we show that due to the nature of multimedia network, the fluctuation in the MAI average causes a threshold drift and thus an increase in the probability of error. This paper also provides a stochastic description of the MAI average amplitude fluctuation using a predefined multimedia probability density function. A system model is presented. From the theoretical analysis and numerical results, it is shown that the proposed system has good performance without dynamic estimation of the detection threshold, thus is independent of both the number of users and the distribution of those users in the offered multimedia classes.**

I. Introduction

LATELY there is a growing interest in the development of broadband optical fiber communication networks for multimedia applications. Such networks must support heterogeneous traffic like high-speed and low-speed data, text, image, audio, and video, with varieties of quality of services (QoS) and traffic requirements [1]-[2].

Optical fast frequency hopping CDMA (OFFH-CDMA) system using fiber Bragg gratings and direct detection has been investigated in [2] and [3]. Due to the unpredictable system activities in [2], the average of the multiple access interference (MAI) will be unpredictable. Because the optimal threshold is a function of the average MAI, it will fluctuate depending on the system activities in terms of the number of users. In multimedia applications, another problem contributes greatly to the dynamic variation of the optimal detection threshold, namely users have the possibility of changing their traffic types dynamically as proposed in [2]. We will show that the average MAI is not only a function of the active number of users, but also on the processing gain (PG), the used power control function, and the distribution of the active users between different multimedia classes.

To solve this problem, we have proposed a new system architecture based on the one proposed in [2]. In this new architecture, each user is assigned two mutually orthogonal two-dimensional code sequences with equal PG. One is designated for "0" transmission and its orthogonal version is used for transmitting data "1". In [4], Equal-weight orthogonal (EWO) signaling was used. The orthogonal sequence was generated using a time-shifted reverse version of the original sequence. On the other hand, in our system the orthogonality between the two versions is achieved by using a frequency-shifted version (FSV) of the original code in a way no frequency overlap exists between the two codes as shown in Fig. 1. This method allows extra degree of flexibility especially in multirate system where codes with different lengths are used and the time-shifted reverse version may lead to higher crosscorrelation and out of phase autocorrelation [1].

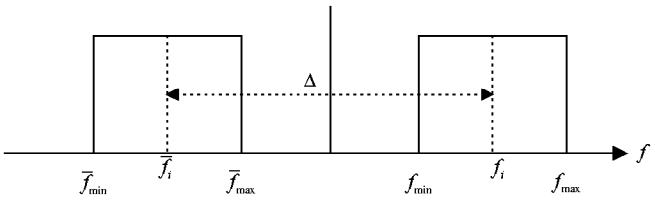

Fig. 1. Bandwidth of the proposed system.

In Section II, we analyze the original system performance using Gaussian assumption where we show the dependence of the optimal threshold on the average MAI. In Section III, we present the modified system based on the FSV of the original system. In addition, we derive its SIR expression using the same technique adopted for the original system but with a simple time-frequency transformation and we show that its performance is independent of the average MAI. In Section IV, we analyze the random fluctuation of the average MAI in a multimedia network and derive a stochastic formula for a newly defined parameter called the threshold drift. In Section V, a numerical simulation is presented. Finally, we conclude in Section VI.

II. Original System

A. System Model

Consider a fiber optic CDMA communication network with transmitter/receiver pairs using OFFH-CDMA [2]. This system supports K users, which share the same optical medium in a star architecture. Each of the K users has the possibility of switching its traffic rate for any of S possible values $R_0 < R_1 < \ldots < R_{S-1}$ corresponding to S different types of multimedia traffic or S different classes. The corresponding PG's are given by $G_0 > G_1 > \ldots > G_{S-1}$ where $G_i = T_i/T_c$. T_i and T_c are the bit period and chip duration,

respectively. The class transmission power is given by $P^{(s)}$ for $s \in \{0,1,...,S-1\}$.

B. *Average* SIR

The derivation to obtain the system SIR is similar to the analysis presented in [5], and thus it will not be fully presented here. Using the model used in [5], the SIR experienced by an active user that has rate R_m is

$$\mathrm{SIR}_m = \frac{G_m^2}{\sum_{k=1}^{K_m-1} \sigma_{m,m}^2 + \sum_{\substack{s=0 \\ s\neq m}}^{S-1} \sum_{k=0}^{K_s-1} \frac{P^{(s)}}{P^{(m)}} \sigma_{m,s}^2 + \sigma_n^2} \tag{1}$$

where $\sigma_{m,j}^2 \ \forall j \in \{0,1,...,S-1\}$ is given by

$$\sigma_{m,j}^2 = \frac{1}{2G_j}\left\{ R_k(G_m,G_j) - \frac{1}{2G_j} J_k^2(G_m,G_j) \right\} \tag{2}$$

In addition, $J_k(G_m,G_j)$ and $R_k(G_m,G_j)$ are the average and correlation parameters [5] (For details, please refer to [5]).

C. *From a Detection Theory Perspective*

Each source generates an output that in the simplest case is one of two choices, which are referred to as hypotheses labeled by H_0 and H_1. In optical CDMA systems H_0 and H_1 correspond to the cases when "zero" and "one" are sent, respectively. In order to detect the desired signal in MAI plus noise, the two above-mentioned hypotheses can be defined as; H_0: *MAI plus noise is received* and H_1: *signal* S_D *plus MAI plus noise is received*. Thus, the decision at the i^{th} receiver, which is tuned to the i^{th} transmitter that transmits using rate R_s and power $P^{(s)}$ is Z_i, which can be treated as a random variable whose statistical properties under both hypotheses are known. To make the detection approach clearer and to show the importance of the detection threshold in the original system, we assume that our detector follows the B procedure [8].

Consider a system with the two hypotheses concerning a real observation Z_i mentioned before

$$\begin{aligned} H_0 &: Z_i = I_m + \mu_0 \\ H_1 &: Z_i = I_m + \mu_1 \end{aligned} \tag{3}$$

where I_m is the total MAI plus the background noise, which is modeled as Gaussian random variable with mean μ_{MAI} and variance σ^2, and they are given by

$$\mu_{MAI} = \sqrt{P^{(m)}} \sum_{k=1}^{K_m-1} J_k[T_m,T_m] + \sum_{\substack{s=0 \\ s\neq m}}^{S-1} \sqrt{P^{(s)}} \sum_{k=0}^{K_s-1} J_k[T_m,T_s] \tag{4}$$

$$\begin{aligned} \sigma^2 = {} & P^{(m)} \sum_{k=1}^{K_m-1} \left(R_k[T_m,T_m] - J_k^2[T_m,T_m] \right) \\ & + \sum_{\substack{s=0 \\ s\neq m}}^{S-1} P^{(s)} \sum_{k=0}^{K_s-1} \left(R_k[T_m,T_s] - J_k^2[T_m,T_s] \right) + \sigma_n^2 \end{aligned} \tag{5}$$

The two parameters μ_0 and μ_1 are fixed numbers given by $\mu_0 = 0$ and $\mu_1 = S_D$. Note that the addition of μ_0 or μ_1 to I_m changes only the mean value of the observation. In terms of distributions on the observation space, the hypothesis pair of (3) can be rewritten as

$$\begin{aligned} H_0 &: Z_i \sim p_0(z_i) = N\left(\mu_0 + \mu_{MAI}, \sigma^2\right) \\ H_1 &: Z_i \sim p_1(z_i) = N\left(\mu_1 + \mu_{MAI}, \sigma^2\right) \end{aligned} \tag{6}$$

where $N(a,b)$ denotes the normal distribution with mean a and variance b. The likelihood ratio statistic [8] for (6) is

$$L(z_i) = \frac{p_1(z_i)}{p_0(z_i)} = \exp\left\{ \frac{S_D}{\sigma_{MAI}^2} \left(z_i - \frac{2\mu_{MAI} + S_D}{2} \right) \right\} \tag{7}$$

As assumed in [5], the data are equiprobable. In addition, we assume uniform cost [8]. Using those constraints, we can define the *Bayes risk* as the overall average cost incurred by a given decision rule π and it is given by

$$r(\pi) = \frac{1}{2}\left\{ 1 + \int_{\Gamma_1} p_0(z_i)\, dz_i - \int_{\Gamma_1} p_1(z_i)\, dz_i \right\} \tag{8}$$

where Γ_1 is the critical region, which is defined by

$$\Gamma_1 = \{ z_i \in \Gamma \mid L(z_i) \geq \eta \} \tag{9}$$

Γ is the observation space and η is equal to one given that we assume equiprobable data and uniform cost.

Due to the fact that $L(z_i)$ is an increasing function of z_i, (9) can be written as

$$\Gamma_1 = \{ z_i \in \Gamma \mid z_i \geq \eta_{opt} \} \tag{10}$$

where η_{opt} is the optimal detection threshold and can be easily shown to be

$$\eta_{opt} = \mu_{MAI} + \frac{S_D}{2} \tag{11}$$

When the system activities change dynamically, the MAI average can be modeled as $m_{MAI} = \mu_{MAI} + \sigma_s$, where σ_s is the threshold drift, which will be estimated in Section IV. Thus, the *Bayes risk* becomes

$$r(\pi) = \frac{1}{2}\left\{ 1 + \Phi\left(-\frac{\sqrt{\mathrm{SIR}}}{2} - \frac{\sigma_s}{\sigma_{MAI}} \right) - \Phi\left(\frac{\sqrt{\mathrm{SIR}}}{2} - \frac{\sigma_s}{\sigma_{MAI}} \right) \right\} \tag{12}$$

Note that if the detector tracks the stochastic variation in the average MAI, $\sigma_s = 0$ and the *Bayes risk* takes on its absolute minimum value, which is given by

$$r_{\min}(\pi) = 1 - \Phi\left(\frac{\sqrt{\text{SIR}}}{2}\right) \tag{13}$$

Fig. 2 shows the *Bayes risk* versus the SIR when we fix the ratio σ_s/σ_{MAI}. It is clear that when σ_s/σ_{MAI} becomes higher the risk of doing an error becomes also higher. In addition, it is normal that when the SIR increases, the risk tends asymptotically to very small values.

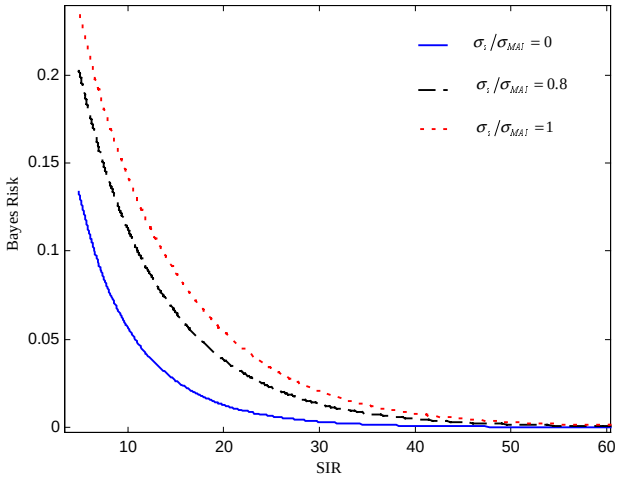

Fig. 2. Bayes risk for the *class-hr* users versus SIR_{hr} and for three different value of σ_s/σ_{MAI}.

III. Modified System

A. System Model

Consider the same fiber optic CDMA communication network used in the previous section with a new transmitter/receiver pair using OFFH-CDMA. Each user is assigned two-mutually orthogonal sequences with equal weight generated from the same family of codes using a FSV as the orthogonal sequence. Fig. 3(a) shows the transmitter architecture using the FSV of the FFH code signaling. It is practically realized by using two encoders, which represent a series of fiber Bragg gratings tuned to the desired user code $a_k^{(s)}(t,f)$ and its orthogonal version $\overline{a}_k^{(s)}(t,f)$. Notice that the over bar means the FSV. The data is fed into the encoders using two wide-band sources. Thus, the data bits are modulated either by the sequence $a_k^{(s)}(t,f)$ or its FSV $\overline{a}_k^{(s)}(t,f)$ depending on whether it is a "1" or a "0", respectively. The two codes are shown in Fig. 3(b) and they are related by $a_k^{(s)}(t,f) = \overline{a}_k^{(s)}(t, f+\Delta)$, where Δ is the frequency shift. In addition, $\overline{f}_{\max}$ must be less then $f_{\min}$.

Fig. 3(c) shows the receiver of the modified system, which is practically realized by a 1:2 coupler and two matched filters. The lower branch filter is a correlator matched to $a_k^{(s)}(t,f)$ and the upper branch filter is matched to $\overline{a}_k^{(s)}(t,f)$. The optical outputs of the two correlators are subtracted via a balanced photodiode. For this system, The transmitted signal $S_k(t,f)$ can be expressed as

$$S_k(t,f) = \sqrt{P^{(s)}}\,\overline{a}_k^{(s)}(t, f + \Delta b_k^{(s)}(t)) \tag{14}$$

where $b_k^{(s)}(t)$ is the baseband unipolar signal, of values {0, 1}, for traffic type *s*. Notice that when the data bit is "0", the transmitted signal is $S_k(t,f) = \sqrt{P^{(s)}}\,b_k^{(s)}(t)a_k^{(s)}(t,f)$. On the other hand when the data bit is "1", the transmitted signal is $S_k(t,f) = \sqrt{P^{(s)}}\,b_k^{(s)}(t)\overline{a}_k^{(s)}(t,f)$. The received signal at each receiver can be written as

$$\begin{aligned} y(t,f) &= \sum_{k=0}^{K-1} S_k(t-\tau_k, f) + n(t) \\ &= \sum_{k=0}^{K-1} \sqrt{P^{(s)}}\,\overline{a}_k^{(s)}(t-\tau_k, f + \Delta b_k^{(s)}(t-\tau_k)) + n(t) \end{aligned} \tag{15}$$

The signal at the output of the adder is averaged over the bit duration T_m by an integrate-and-dump low pass filter. Therefore, the decision variable at the filter output is

$$\begin{aligned} Z_0^{(m)} = N + \frac{1}{(1+\alpha)} \sum_{s=0}^{S-1} \sum_{k=0}^{K_s-1} \int_o^{T_m} & S_k(t-\tau_k, f) \\ & .\left[a_0^{(m)}(t,f) - \alpha\overline{a}_0^{(m)}(t,f)\right] dt \end{aligned} \tag{16}$$

where N is a zero-mean AWGN with variance $\sigma_n^2 = N_0 T_m / 4$ and T_m is the bit period corresponding to rate R_m.

In order to eliminate the frequency dimension of the signals we use the Hamming correlation concept used in [5], which enables us to write (16) as

$$\begin{aligned} Z_0^{(m)} = N & \\ + \frac{1}{(1+\alpha)} \sum_{s=0}^{S-1} \sum_{k=0}^{K_s-1} \int_o^{T_m} & \sqrt{P^{(s)}}\,h\left(\overline{a}_k^{(s)}(t-\tau_k) + \Delta b_k(t-\tau_k), a_0^{(m)}(t)\right) dt \\ - \frac{\alpha}{(1+\alpha)} \sum_{s=0}^{S-1} \sum_{k=0}^{K_s-1} \int_o^{T_m} & \sqrt{P^{(s)}}\,h\left(\overline{a}_k^{(s)}(t-\tau_k) + \Delta b_k(t-\tau_k), \overline{a}_0^{(m)}(t)\right) dt \end{aligned} \tag{17}$$

The sequences $a_k^{(s)}(t)$, $\overline{a}_k^{(s)}(t)$, $a_0^{(m)}(t)$, and $\overline{a}_0^{(m)}(t)$ are real numbers representing the hopping frequencies along with their orthogonal versions used at time *t* for the k^{th} interferer and the desired user, respectively.

B. Average SIR

Using this modified model, the desired signal component, assuming perfect synchronization between the receiver and the desired transmitter and balanced coupler, thus $\alpha = 1$, is

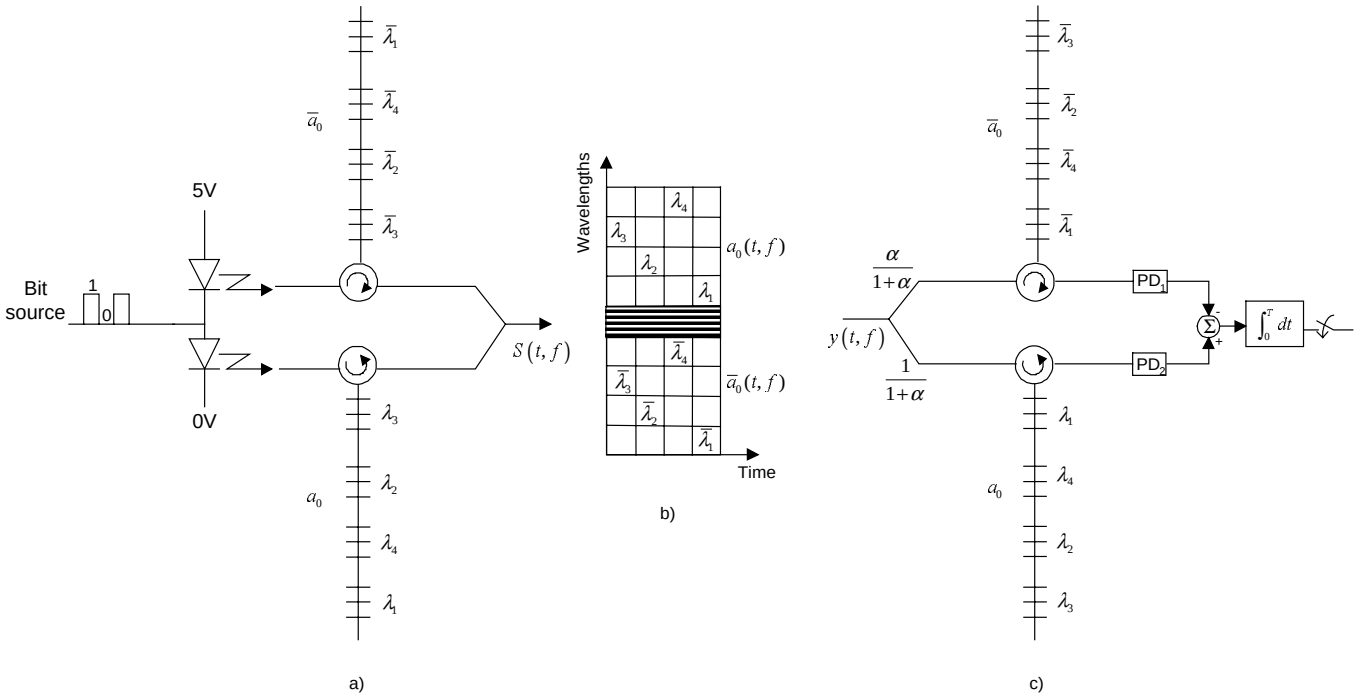

Fig. 3. a) Modified OFFH-CDMA transmitter, b) its corresponding 2D-code structure, and c) Modified OFFH-CDMA receiver.

$S_D = \pm\sqrt{P^{(m)}}T_m/2$ for $b_0^{(m)} = 1$ and $b_0^{(m)} = 0$, respectively. The MAI I_k from user k that transmits data with rate R_s is

$$I_k = \frac{\sqrt{P^{(s)}}}{(1+\alpha)}\int_o^{T_m} h\left(\overline{a}_k^{(s)}(t-\tau_k)+\Delta b_k(t-\tau_k), a_0^{(m)}(t)\right)dt - \frac{\alpha\sqrt{P^{(s)}}}{(1+\alpha)}\int_o^{T_m} h\left(\overline{a}_k^{(s)}(t-\tau_k)+\Delta b_k(t-\tau_k), \overline{a}_0^{(m)}(t)\right)dt \quad (18)$$

I_k is assumed to be an independent random variable. Its variance can be written as $\sigma_{I_k}^2 = E(I_k^2) - E^2(I_k)$, where $E(.)$ is the expectation operator. We assume that τ_k and $b_k^{(s)}(t)$, for $1 \le k \le K$, are mutually independent. τ_k is uniformly distributed over the range $0 \le \tau_k \le T_s$ and $\Pr\left[b_k^{(s)} = 1\right] = \Pr\left[b_k^{(s)} = 0\right] = 1/2$. Thus, averaging over τ_k and $b_k^{(s)}$, we obtain

$$E(I_k) = \sqrt{P^{(s)}}J_k[T_m, T_s]$$

$$E(I_k^2) = P^{(s)}R_k[T_m, T_s]$$

where $J_k[T_m, T_s]$ and $R_k[T_m, T_s]$ are the average and correlation parameters, respectively, and they must be derived for two different cases: 1) $T_m \le T_s$ and 2) $T_m > T_s$.

1) $T_m \le T_s$

Averaging over all possible values of $b_{k,-1}^{(s)}$ and $b_{k,0}^{(s)}$, we will get

$$J_k[T_m, T_s] = \frac{(1-\alpha)}{(1+\alpha)}\frac{1}{2T_s}\int_0^{T_s} H_{k,0}(0, T_m)d\tau_k \quad (19)$$

$$R_k[T_m, T_s] = \frac{(1+\alpha^2)}{(1+\alpha)^2}\frac{1}{2T_s}\int_0^{T_m} H_{k,0}^2(0,\tau_k) + H_{k0}^2(\tau_k, T_m)d\tau_k + \frac{(1+\alpha^2)}{(1+\alpha)^2}\frac{1}{2T_s}\int_{T_m}^{T_s} H_{k,0}^2(0, T_m)d\tau_k + \frac{(1-\alpha)}{(1+\alpha)^2}\frac{1}{2T_s}\int_0^{T_m} H_{k,0}(0,\tau_k)H_{k,0}(\tau_k, T_m)d\tau_k \quad (20)$$

where $H_{k,0}(0,\tau_k)$, $H_{k,0}(\tau_k, T_m)$ and $H_{k,0}(0, T_m)$ are given by

$$H_{k,0}(\tau_i, \tau_j) = \int_{\tau_i}^{\tau_j} h(a_k(t-\tau_k), a_0(t))dt$$

2) $T_m > T_s$

By taking $L = \lfloor (T_m - \tau_k)/T_s \rfloor$ and averaging over all possible values of the overlapping bits $b_{k,-1}^{(s)}, \ldots, b_{k,L}^{(s)}$, $J_k[T_m, T_s]$ and $R_k[T_m, T_s]$ are given by (21) and (22), respectively.

$$J_k[T_m, T_s] = \frac{(1-\alpha)}{(1+\alpha)}\frac{1}{2T_s}\int_0^{T_s} H_{k,0}(0, T_m)d\tau_k \quad (21)$$

$$R_k[T_m,T_s]=$$
$$\frac{(1+\alpha^2)}{(1+\alpha)^2}\frac{1}{2T_s}\int_0^{T_s}\Big[H_{k,0}^2(0,\tau_k)+H_{k,0}^2(\tau_k+LT_s,T_m)+\sum_{y=1}^{L}H_{k,0}^2(\tau_k+(y-1)T_s,\tau_k+yT_s)\Big]d\tau_k$$
$$+\frac{(1-\alpha)}{(1+\alpha)^2}\frac{1}{2T_s}\int_0^{T_s}\Big[H_{k,0}(0,\tau_k)H_{k,0}(\tau_k+LT_s,T_m)+(H_{k,0}(0,\tau_k)+H_{k,0}(\tau_k+LT_s,T_m))H_{k,0}(\tau_k,LT_s)+\frac{1}{2}\sum_{x=1}^{L}\sum_{\substack{y=1\\y\neq x}}^{L}H_{k,0}(\tau_k+(y-1)T_s,\tau_k+yT_s).H_{k,0}(\tau_k+(x-1)T_s,\tau_k+xT_s)\Big]d\tau_k \quad (22)$$

By considering a balanced coupler ($\alpha=1$) and using the discrete partial-period aperiodic hamming-correlation functions defined in [5], $J_k[T_m,T_s]$ becomes equal to zero and $R_k[T_m,T_s]$ will be

$$R_k[T_m,T_s]=\begin{cases}\frac{T_c^3}{4T_s}\Big\{\sum_{q=0}^{G_m-1}\big[AH_1^2(q)+AH_2^2(q,G_m)\big]+\sum_{q=G_m}^{G_s-1}AH_3^2(q,G_m)\Big\}, & T_m\le T_s\\ \frac{T_c^3}{4T_s}\sum_{q=0}^{G_s-1}\Big[AH_1^2(q)+AH_2^2(q+LG_s,G_m)+\sum_{y=1}^{L}AH_4^2(q,y,G_s)\Big], & T_m>T_s\end{cases} \quad (23)$$

Therefore, the mean of the MAI vanishes to zero independently of the active number of users or the classes chosen by those users. In addition, the cross terms in (20) and (22) are forced to be equal to zero. Thus, the above result is consistent with the one obtained in [6] for coherent multirate DS-CDMA.

If we define $R_k[G_m, G_s] = R_k[T_m, T_s]/(T_c^2/4G_s)$, the SIR experienced by an active user that has rate R_m and using the modified system is the same as the one defined in (1) but the variance $\sigma_{m,j}^2\ \forall j\in\{0,1,...,S-1\}$ is now given by

$$\sigma_{m,j}^2=\frac{1}{2G_j}R_k\left[G_m,G_j\right] \quad (24)$$

IV. Stochastic Amplitude Fluctuation of the Average MAI

This section provides a stochastic description of the MAI amplitude fluctuation using a predefined multimedia probability density function (pdf). Because every user may choose his class and modify it dynamically, we assume that the *class-s* can be considered as a discrete random variable with a certain probability mass function (pmf) given by $P_s=\Pr(\text{user k choses the } class\text{-}s)$ with $\sum_{s=0}^{S-1}P_s=1$

Proposition 1: Given that the sequences used for each class respects the one coincidence criteria, the expected value of the average MAI generated from the k^{th} user that transmits using the *class-s* is given by

$$\mu_{I_k}(s)=\frac{T_c}{2}\sqrt{P^{(s)}}\left(\frac{G_m}{F}\right) \quad (25)$$

where, F is the total number of available frequencies.

Proof: The proof is omitted due to the limited space. ■

Due to the fact that we have considered the *class-s* as being a random variable, $\mu_{I_k}(s)$ is also a random variable with mean m and variance δ^2, which can be written as

$$m=E_s\left(\mu_{I_k}(s)\right)=\frac{T_c}{2}\left(\frac{G_m}{F}\right)\left(\sum_{s=0}^{S-1}P_s\sqrt{P^{(s)}}\right) \quad (26)$$

$$\delta^2=E_s\left(\mu_{I_k}^2(s)\right)-m^2=\left(\frac{T_c}{2}\right)^2\left(\frac{G_m}{F}\right)^2\left\{\sum_{s=0}^{S-1}P_sP^{(s)}-\sum_{s=0}^{S-1}\sum_{t=0}^{S-1}P_sP_t\sqrt{P^{(s)}P^{(t)}}\right\} \quad (27)$$

Since the users are assumed independent and may choose their classes also independently from each other, the mean, M_s, and the variance, σ_s^2, of the total MAI average are the sum of the means and variances from all active users respectively, and they are given by

$$M_s=(K-1)m \quad (28)$$

$$\sigma_s^2=(K-1)\delta^2 \quad (29)$$

In this paper, the MAI average fluctuation is regarded as the square root of the variance or the standard deviation from the mean σ_s. The variable σ_s is a measure of the amount of threshold drift and we call it the threshold line width. The optimum threshold level given in (11) contains two terms. The second term is the average MAI and the fluctuation of this term causes the amplitude fluctuation in the detection threshold. Thus it induces a drift from the optimal threshold. Therefore, we can model the detection threshold at the receiver as follows

$$\eta=\frac{S_D}{2}+\mu_{MAI}\pm\sigma_s \quad (30)$$

From (30), we can notice that the threshold drift is greatly dependent on the total number of users, the multimedia distribution and the applied power control function.

In Fig. 4 and Fig. 5 we plot the BER versus the detection threshold for the case of two class system namely *class-hr* and *class-lr*, respectively, and using extended hyperbolic

congruential (EHC) family of codes [7] with $F = 41$ available frequencies. One can notice clearly the dependence of the BER and the η_{opt} on the PG of the desired user, the transmission power and the multimedia pdf adopted in the network, assuming fixed number of users ($K = 12$). In these figures, $P_s = [P_{lr} \;\; P_{hr}]$ and $P^{(s)} = [P^{(lr)} \;\; P^{(hr)}]$ represent vectors containing the pmf and the transmission power of each class, respectively. We can observe the variation of η_{opt} when we vary the transmission power of the two classes. Therefore, in a multirate system, the optimal threshold will fluctuate not only with the number of active users, but also with the optimal power control function, which assigns a given transmission power for each class in order to maximize the system throughput as shown in [2].

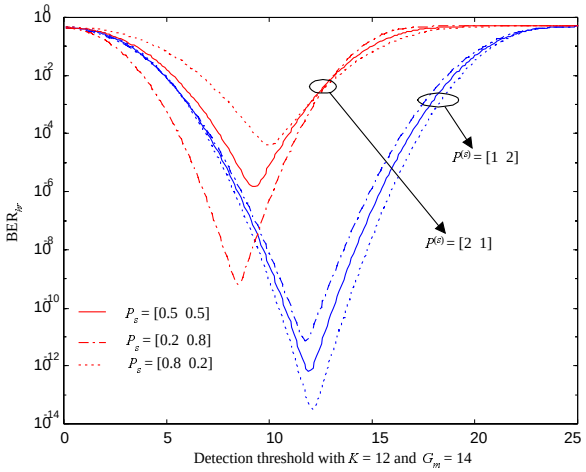

Fig. 4. *class-hr* BER versus the detection threshold for $K = 12$.

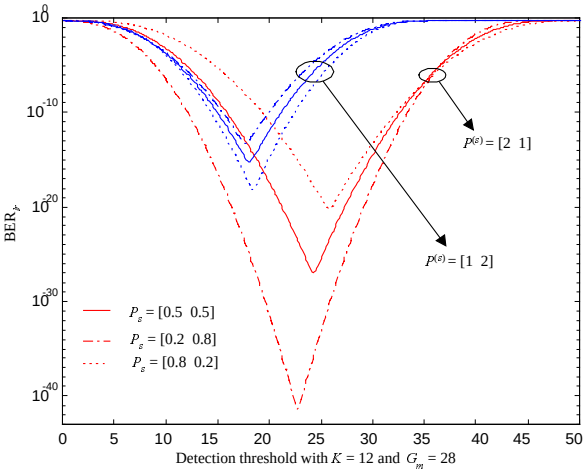

Fig. 5. class-*lr* BER versus the detection threshold for $K = 12$.

V. Numerical Results and Discussions

Throughout this section, it must be noted that the same family of codes used previously is employed. Moreover, the power control algorithm and the definition of throughput are used according to [2]. The quality of service guaranties (QoS) for each class are taken to be a lower bound on the SIR. Fig. 6 and Fig. 7 show the BER performance comparison, between the two systems, for a *class-hr* and a *class-lr* users, respectively, and using a multimedia pdf of $P_{hr} = P_{lr} = 0.5$ while varying the power ratio $P^{(lr)}/P^{(hr)}$ to take values 3/4 and 1/2. It is clear that in both cases, the BER of the original system is better than that of the modified one when the detector tracks the optimal threshold. Note that when the number of users becomes high, the two BERs become closer. Observe also that for a lower rate user, the difference between the performances of the two systems is wider than for a higher rate user.

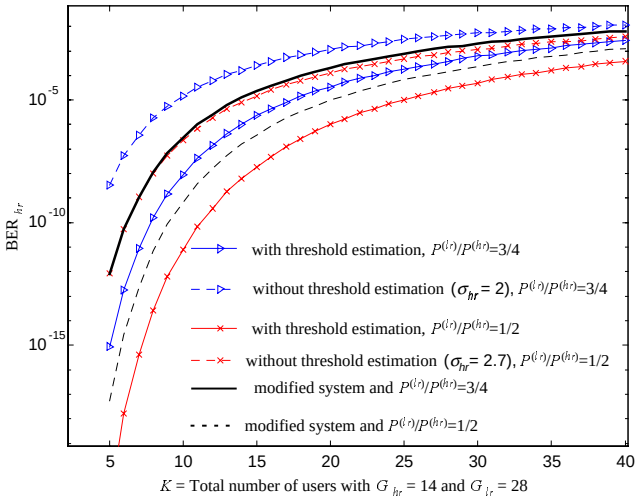

Fig. 6. *class-hr* BER versus the total number of users, for the original and the modified systems.

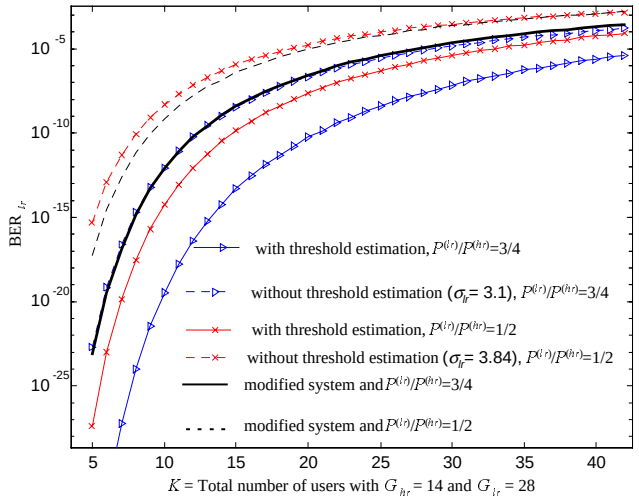

Fig. 7. *class-lr* BER versus the total number of users, for the original and the modified systems.

When the detector does not track the optimal threshold, thus inducing a threshold drift, the BER of the modified

system is observed to be better than that of the original one for the two classes and for the two values of $P^{(lr)}/P^{(hr)}$. The threshold drift for a *class-hr* user is $\sigma_{hr} = 2$ when $P^{(lr)}/P^{(hr)} = 3/4$ and $\sigma_{hr} = 2.7$ when $P^{(lr)}/P^{(hr)} = 1/2$. On the other hand the threshold drift for a *class-lr* user is $\sigma_{lr} = 3.35$ when $P^{(lr)}/P^{(hr)} = 3/4$ and $\sigma_{hr} = 3.84$ when $P^{(lr)}/P^{(hr)} = 1/2$. Therefore, the drift increases as the power ratio deceases.

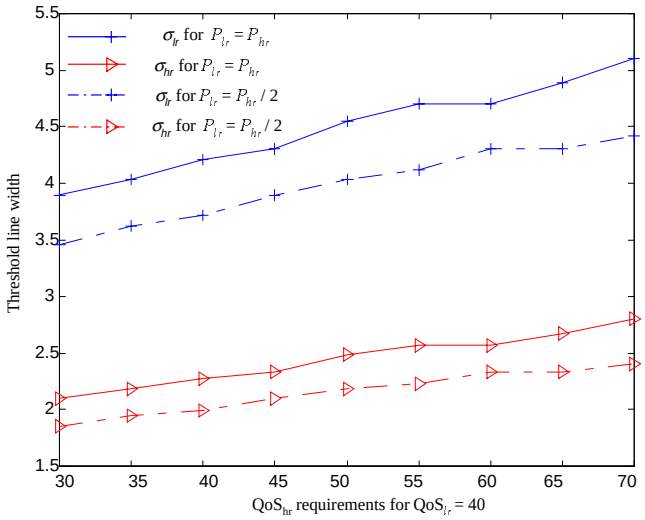

Fig. 8. Threshold line width versus the *class-hr* QoS requirement, for fixed *class-lr* QoS of 40.

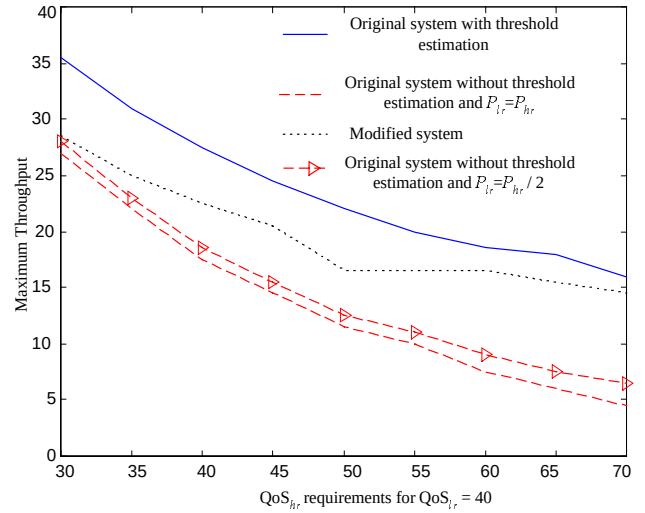

Fig. 9: Maximum throughput for the original and the modified systems versus the *class-hr* QoS requirement, and for fixed *class-lr* QoS of 40.

In Fig. 8, we plot the threshold line width versus the QoS guaranties for the *class-hr* QoS_{hr}, when power control is used and for fixed QoS_{lr}. Notice that the drift for *class-hr* users is smaller than that of *class-lr* users. When QoS_{hr} increases, σ_{hr} and σ_{lr} also increase. Observe that when we vary the multimedia pdf from $P_{hr} = P_{lr}/2$ to $P_{hr} = P_{lr}$, the drift increases for the two classes.

Using the results shown in Fig. 8, Fig. 9 illustrates a comparison between the throughput of the original and the modified system when power control is used and when we vary the QoS_{hr}. Simulation shows that the throughput of the original system is always higher than that of the modified system when the detector tracks the variations in the optimal threshold. On the other hand, the throughput of the modified system is better than that of the original one when the detector does not track the variations in the optimal threshold. Moreover, when we change the multimedia pdf from $P_{hr} = P_{lr}/2$ to $P_{hr} = P_{lr}$, the throughput of the original system decreases due to the fact that the drift increases for the two classes.

VI. Conclusion

The average MAI fluctuation in a multirate OFFH-CDMA system has been described given a pre-specified multimedia distribution and a power control function. These fluctuations cause a drift in the optimal detection threshold, which was estimated theoretically and quantified as a variable called threshold line width. To solve this problem, a new multirate OFFH-CDMA system was proposed. The SIR and the BER was evaluated for the new system using a FSV of the codes used in the original system. Results demonstrated that the new system achieves good performance without dynamic estimation of the receiver threshold. As a conclusion, this new system architecture is recommended for multirate-multimedia applications.

VII. References

[1] J. G. Zhang, "Flexible Optical CDMA Networks Using Strict Optical Orthogonal Codes for Multimedia Broadcasting and Distribution Applications," *IEEE Trans. On broadcasting*, vol. 45, pp. 106-115, March 1999.

[2] E. Inaty, L. A. Rusch, and P. Fortier, "Multirate Optical Fast Frequency Hopping CDMA System Using Power Control," in *proc. IEEE Globecom 2000*, San Francisco, CA, vol. 2, pp. 1221-1228, November 2000.

[3] H. Fathallah, L. A. Rusch and S. Larochelle, "Passive Optical Fast Frequency Hop CDMA Communication System," *IEEE J. on Lightwave Technology*, vol. 17, pp. 397-405, March 1999.

[4] T. Ohtsuki, "Performance Analysis of Direct-Detection Optical CDMA Systems with Optical Hard-Limiter Using Equal-Weight Orthogonal Signaling," *IEICE Trans. on communications*, vol. E82-B, NO.3, pp. 512-520, March 1999.

[5] E. Inaty, P. Fortier, and L. A. Rusch "SIR Performance Evaluation of a Multirate OFFH-CDMA System," *IEEE Comm. Letters*, vol.5, no. 5, pp.224-226, April 2001.

[6] T. Ottosson and A. Svensson, "Multi-rate performance in DS/CDMA system," *Tech. Report no.* 14, ISSN 0283-1260, Dept. of Information Theory, Charlmers University of Technology, Göteborg, Sweden, March 1995.

[7] L. D. Wronski, R. Hossain, and A. Albicki, "Extended hyperbolic congruential frequency hop code: Generation and bounds for cross- and auto-ambiguity function," *IEEE Trans. on Communications*, vol. 44, no. 3, pp. 301-305, April 1996.

[8] Van Trees, H. L. *Detection, Estimation and Modulation Theory, Part I*, 1968, Wiley, New York.